

6.6.2 Phasor Diagrams for Salient-Pole Machines

The inductive effects of the direct- and quadrature -axis armature flux waves can be accounted for by *direct- and quadrature-axis magnetizing reactances*, X_{ad} and X_{aq} , respectively, similar to the magnetizing reactance X_a of cylindrical -rotor theory. These reactances account for the inductive effects of the space-fundamental air-gap fluxes created by the armature currents along the direct and quadrature axes, $\dot{\Phi}_{ad}$ and $\dot{\Phi}_{aq}$ respectively. Because of the longer air gap between the poles and the corresponding larger reluctance, the space-fundamental armature flux when the armature mmf is aligned with the quadrature axis is less than the space fundamental armature flux which would be created by the same armature current if the armature mmf wave were aligned with the direct axis. Hence, the quadrature-axis magnetizing reactance is less than that of the direct axis.

With each of the component currents \dot{I}_d and \dot{I}_q there is associated a component synchronous-reactance voltage drop, $j\dot{I}_d X_d$ and $j\dot{I}_q X_q$ respectively. The reactances X_d and X_q are, respectively, the *direct- and quadrature-axis synchronous reactances* and are equal to the sum of the direct- and quadrature-magnetizing reactances and the armature-winding leakage reactance. The direct- and quadrature axis synchronous reactances are then given by

$$X_d = X_{ad} + X_\sigma \quad (1)$$

$$X_q = X_{aq} + X_\sigma \quad (2)$$

where X_σ is the armature leakage reactance, assumed to be the same for direct-and quadrature-axis currents. As we have discussed, the quadrature axis synchronous reactance X_q is less than that of the direct axis X_d because of the greater reluctance of the longer air gap in the quadrature axis. Note that a small salient-pole effect is present even in cylindrical-rotor turbo-alternators because of the effect of the slots for the field winding on the rotor quadrature-axis.

As shown in the generator phasor diagram of Fig. 1, the generated voltage \dot{E}_0 equals the phasor sum of the terminal voltage \dot{U} plus the armature resistance drop $\dot{I}R_a$ and the component synchronous-reactance drops $j\dot{I}_d X_d + j\dot{I}_q X_q$.

$$\dot{E}_0 = \dot{U} + \dot{I}R_a + j\dot{I}_d X_d + j\dot{I}_q X_q \quad (3)$$

From this phasor diagram we also see that, given the power-factor angle φ and the power angle δ , the magnitude of the component currents can be found as

$$I_d = I \sin(\delta + \varphi) = I \sin \psi_0 \quad (4)$$

$$I_q = I \cos(\delta + \varphi) = I \cos \psi_0 \quad (5)$$

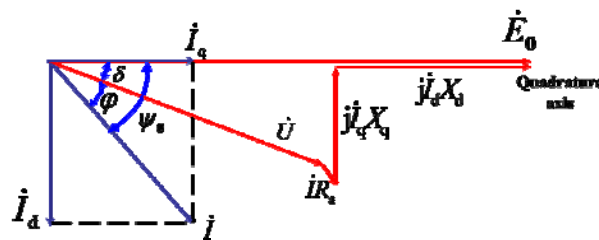


Figure 1 Phasor diagram for a synchronous generator showing the relationship between the voltages and the currents

The phasor diagram of Fig. 1 is drawn for the case of a lagging power factor and hence the angle φ as drawn has a positive value.

Just as for the synchronous reactance X_s of a cylindrical-rotor machine, the reactances X_d and X_q are not constant with flux density but rather saturate as the machine flux density increases. It is common to find both unsaturated and saturated values specified for each of these parameters. The saturated values apply to typical machine operating conditions for which the terminal voltage is near its rated value. For our purposes in this chapter and elsewhere in this book, we will not focus attention on this issue and, unless specifically stated, the reader may assume that the values of X_d and X_q given are the saturated values.

In drawing a phasor diagram such as that of Fig.1, the armature current must be resolved into its direct- and quadrature-axis components. This resolution assumes that the phase angle $\delta + \varphi$ of the armature current with respect to the generated voltage is known. Typically, however, although the power-factor angle φ at the machine terminals is known, the angle δ between the terminal voltage and the generated voltage is not known. It is thus necessary to locate the quadrature axis and to compute δ .

A portion of the phasor diagram of Fig.1 is repeated in Fig. 2. Note that in this case, instead of adding the phasors $j\dot{I}_dX_d$ and $j\dot{I}_qX_q$ to the tip of the phasor $\dot{I}R_a$, the figure shows the addition of the phasors $j\dot{I}_dX_q$ and $j\dot{I}_qX_q$. Although the phasor $j\dot{I}_dX_q$ is somewhat shorter than the phasor $j\dot{I}_dX_d$ of Fig.1, both are parallel to the quadrature axis and hence in each case, the addition of the phasor $j\dot{I}_qX_q$ results in a phasor which terminates on the quadrature axis.

The key point of the phasor diagram of Fig. 2 is that, $j(\dot{I}_d + \dot{I}_q)X_q = j\dot{I}X_q$ and thus **the quadrature axis can be located by adding the phasor $j\dot{I}X_q$ to the phasor $\dot{U} + \dot{I}R_a$** . Once the quadrature axis (and hence δ) is known, \dot{I}_d and \dot{I}_q can be determined and the generated voltage \dot{E}_0 can be found from Eq.3.

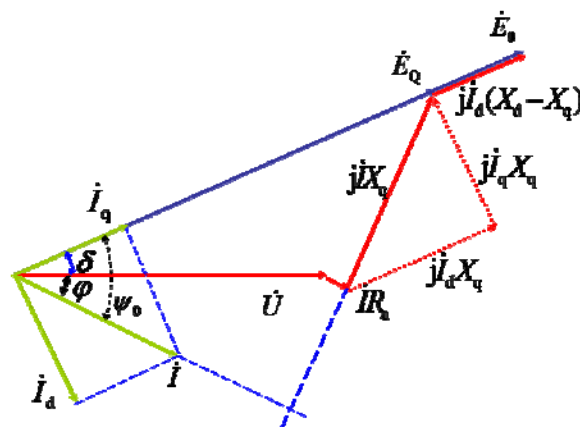


Figure 2 Phasor diagram illustrating the technique for locating the quadrature axis

6.7 POWER-ANGLE CHARACTERISTICS OF SALIENT-POLE MACHINES

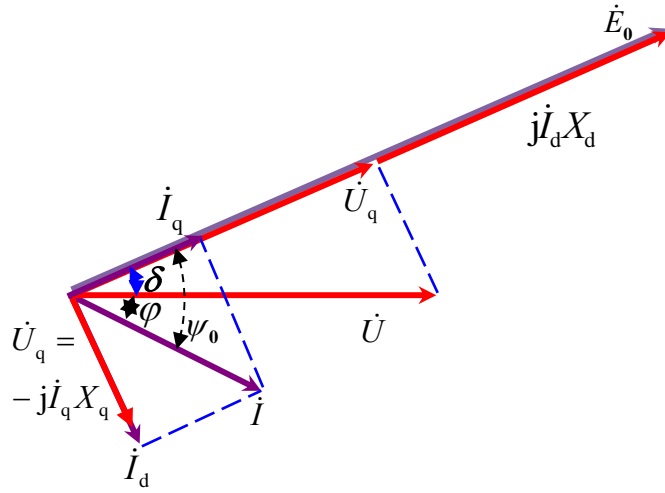


Figure 3 Phasor diagram illustrating the direct and quadrature axis components of Eq. 6

For the purposes of this section, we will consider a synchronous machine acting as a generator and will neglect the armature resistance R_a because it is usually small. With R_a neglected, Eq. 3 can be rewritten in terms of the direct- and quadrature-axis voltage and current components as

$$\dot{E}_0 = \dot{U}_d + \dot{U}_q + \dot{I}R_a + j\dot{I}_d X_d + j\dot{I}_q X_q \quad (6)$$

Recognizing that the phasors \dot{E}_0 and $j\dot{I}_d X_d$ lies along the quadrature axis and $j\dot{I}_q X_q$ lies along the direct axis, we can re-write Eq. 6 in terms of the magnitudes of its direct- and quadrature -axis components as

Direct axis:

$$0 = U_d - X_q I_q \quad (7)$$

Quadrature axis:

$$E_0 = U_q + I_d X_d \quad (8)$$

These relationships are illustrated in the phasor diagram of Fig. 3. Note that Eqs. 6 through 8 are based upon the generator reference for current.

The generator output power can be calculated as

$$\begin{aligned} P_e &\approx mUI \cos(\psi_0 - \delta) = mUI(\cos \psi_0 \cos \delta + \sin \psi_0 \sin \delta) \\ &= mU(I_q \cos \delta + I_d \sin \delta) \end{aligned} \quad (9)$$

From the phasor diagram of Fig. 3, I_d and I_q can be written in terms of their axis-component magnitudes and the power-angle δ as

$$I_q = U \sin \delta / X_q \quad (10)$$

$$I_d = \frac{(E_0 - U \cos \delta)}{X_d} \quad (11)$$

Substitution into Eq. 9 then gives

$$P_e = m \frac{E_0 U}{X_d} \sin \delta + m \frac{U^2}{2} \left(\frac{1}{X_q} - \frac{1}{X_d} \right) \sin(2\delta) \quad (12)$$

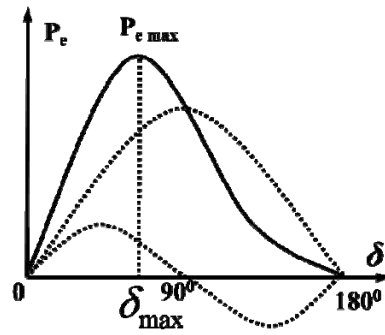


Figure 4 Power-angle characteristic of a salient-pole synchronous machine showing the fundamental component due to field excitation and the second-harmonic component due to reluctance torque

The general form of this power angle characteristic is shown in Fig 4. The first term is the same as the expression obtained for a cylindrical-rotor machine. The second term includes the effect of salient poles. It represents the fact that the air-gap flux wave creates torque, tending to align the field poles in the position of minimum reluctance. This term is the power corresponding to the *reluctance torque*. Note that the reluctance torque is independent of field excitation. Also note that, if $X_d = X_q$ as in a uniform air-gap machine, there is no preferential direction of magnetization, the reluctance torque is zero, and Eq. 12 reduces to the power angle equation for a cylindrical-rotor machine.

Notice that the characteristic for negative values of δ is the same except for a reversal in the sign of P_e . That is, the generator and motor regions are identical if the effects of resistance (not included in the derivation of Eq.12) are negligible.